Table 1 Combustion properties of the propellants

Propellant system	Oxidizer (wt%)	C_p [a] (cal/g°C)	T_s^6 (°C)	Q(condensed phase) (cal/g)	Burning rate[6] at 25°C (cm/sec)
P. F./ammonium perchlorate	77.5	0.30	840	244	0.181
P. F./potassium perchlorate	75	0.24	605	139	0.275
P. F./sodium perchlorate	73.5	0.29	680	190	0.307
P.F./potassium nitrate	75	0.26	510	126	0.453

[a] The specific heat of propellant was assumed to be (¾ C_p oxidizer + ¼ C_p P. F. polymer); C_p at 25°C of ammonium perchlorate is taken from Ref. 7, of potassium nitrate, sodium nitrate, and P. F. polymer from Ref. 8, and of potassium perchlorate from Ref. 9.

(2) that T_s is the temperature (extrapolated) at which the burning rate would become infinite. Thus the T_s measured in our experiments should be identical with T_s' used in Adams[7] theory.

Discussion

Since the specific heats of these propellants at different temperatures are not known, the values at 25°C were used in the present computation. Further assuming an initial temperature of 25°C, heats of reaction in the solid phase of the propellants were calculated using Eq. (1). The condensed phase heats of reaction along with some other burning characteristics of the propellants are given in Table 1. Since the condensed phase reactions are initiated at comparatively higher temperatures, the significant heat of generation does not occur in the experimental temperature range 10-75°C used for the extrapolation of T_s.

It can be seen from the table that for both the nitrate and the perchlorate types propellant burning rate is inversely related to the condensed phase heat of reaction. This shows that it is the pyrolysis kinetics, but not the heat of the exothermic reactions in solid phase, which is significant in controlling the burning rate of composite propellant at low pressures.

Conclusions

The condensed phase heats of reaction of phenol-formaldehyde composite propellants have been computed. These show no relevant connection with the burning rate at atmospheric pressure.

References

[1] Morisaki, S. and Komamiya, K., "Differential Thermal Analysis and Thermogravimetry of Ammonium Perchlorate at Pressure up to 51 Atm," *Thermochimica Acta*, Vol. 12, 1975, pp.239-251.

[2] Rastogi, R. P., Kishore, K., and Gurdip, Singh, "Combustion of Polystyrene and Oxygen-Styrene Copolymer/Ammonium Perchlorate Propellants," *AIAA Journal*, Vol. 12, Jan. 1974, pp. 9-10.

[3] Kirby, C. E. and Suh, N. P., "An Experimental Method for Determining the Condensed Phase Heat of Reaction of Double-Base Propellants," *AIAA Journal*, Vol. 9, April 1971, pp. 754-756.

[4] Adams, G. K., "The Chemistry of Solid Propellant Combustion: Nitrate Ester of Double-Base Systems," *Proceedings of the 4th Symposium on Naval Structural Mechanics*, Purdue Univ., Lafayette, Ind., April 1965, pp. 117-147.

[5] Suh, N. P., Tsai, C. L., Thomson Jr., C. L. and Moore, J. S., "Ignition and Surface Temperature of Double-Base Propellants at Low Pressure: I-Thermocouple Measurements," *AIAA Journal*, Vol. 8, July 1970, pp. 1314-1321.

[6] Girdhar, H. L. and Arora A. J., "Combustion of Phenol Formaldehyde Composite Propellants," *Journal of Spacecraft and Rockets*, Vol. 13, July 1976, pp. 443-445.

[7] Salzman, P. K., Irwin, O. R., and Anderson, W. H., "Theoretical Detonation Characteristics of Solid Composite Propellants," *AIAA Journal*, Vol. 3, Dec. 1965, pp. 2230-2238.

[8] Lange, N. A., *Hand Book of Chemistry*, McGraw Hill, N. Y., 1967, pp. 873, 1529.

[9] Schumacher, C. J., *Perchlorates-Their Properties, Manufacture and Uses*, Reinhold Publishing Corp., N. Y., 1960, p. 30.

Discontinuous Solutions of Three-Dimensional Compressible Stagnation Point Boundary Layers

Margaret Muthanna* and G. Nath†
Indian Institute of Science, Bangalore, India

Introduction

RECENT developments in space flight have focused attention on the problem of predicting the flowfield on general three-dimensional bodies. The steady laminar compressible three-dimensional forward stagnation-point flow of a gas with constant or variable $\rho\mu$ flows (where ρ and μ are the density and viscosity, respectively) both for nodal ($C=b/a \geq 0$, where a and b are velocity gradients at the stagnation point in the x and y directions, respectively) and saddle ($C<0$) points of attachment has been studied by several authors.[1-3] For constant $\rho\mu$ flows ($\rho \propto T^{-1}$, $\mu \propto T$, $Pr=0.7$, where T and Pr are the temperature and Prandtl number, respectively), Libby[1] found two branches of solutions, namely, continuous and discontinuous branches when $C<0$. He observed that the discontinuous branch solutions have certain interesting features that are not found in continuous branch solutions. For example, the transverse profiles for the discontinuous branch have both reverse flow and velocity overshoot for certain critical values of the saddle points of attachment and mass injection, whereas, for the continuous branch, they have only reverse flow but no velocity overshoot. The physical significance of the discontinuous solution when $C \to 0^-$ is that it may represent the flow due to a "wall jet" directed inward along the y axis on a two-dimensional cylinder.[1] For variable gas properties ($\rho \propto T^{-1}$, $\mu \propto T^{\omega}$, $Pr=0.7$, where ω is the index of the power-law variation of viscosity), the discontinuous branch solutions have not been obtained before. However, the continuous branch solutions have been studied by Wortman et al.[2] and Vimala and Nath.[3]

The aim of the present analysis is to obtain the discontinuous branch solutions of the preceding problem with variable gas properties and mass injection for a saddle point of attachment ($-1<C<0$).

Governing Equations

The governing differential equations in dimensionless form for the steady laminar compressible boundary-layer flow with mass injection of a gas with variable properties in the neigh-

Received June 21, 1976; revision received Sept. 7, 1976.
Index category: Boundary Layers and Convective Heat Transfer – Laminar.

*Research Student, Dept. of Applied Mathematics.
†Associate Professor, Dept. of Applied Mathematics.

Table 1 Skin-friction and heat transfer parameters for $Pr = 0.7$ (discontinuous branch)

			$g_w = 0.2$			$g_w = 0.6$		
C	f_w	ω	$f_1''(0)$	$F_1''(0)$	$G'(0)$	$f_1''(0)$	$F_1''(0)$	$G'(0)$
−0.25	0	1.0	0.6172	1.3773	0.4289	0.9189	1.6832	0.4597
	0	0.7	0.7076	1.5825	0.4613	0.9741	1.7783	0.4767
	0	0.5	0.7813	1.7435	0.4887	1.0139	1.8460	0.4885
	−0.25	1.0	0.4865	0.8372	0.2976	0.7928	1.0847	0.3426
	−0.25	0.7	0.5796	1.0135	0.3461	0.8514	1.1738	0.3615
	−0.25	0.5	0.6645	1.1639	0.3749	0.8927	1.2372	0.3746
	−0.5	1.0	0.3720	0.4425	0.1935	0.6813	0.6233	0.2415
	−0.5	0.7	0.4783	0.6366	0.2392	0.7412	0.7050	0.2608
	−0.5	0.5	0.5554	0.8065	0.2864	0.7835	0.7645	0.2740
−0.5	0	1.0	0.6541	0.3599	0.4865	0.9457	0.3503	0.5258
	0	0.7	0.7489	0.4176	0.5285	1.0017	0.3721	0.5448
	0	0.5	0.8224	0.4698	0.5577	1.0413	0.3879	0.5579
	−0.25	1.0	0.5210	0.1661	0.3565	0.8189	0.1281	0.4068
	−0.25	0.7	0.6244	0.2063	0.4074	0.8772	0.1431	0.4284
	−0.25	0.5	0.7052	0.2395	0.4450	0.9185	0.1541	0.4432
	−0.5	1.0	0.4130	−0.0155	0.2583	0.7088	−0.0608	0.3132
	−0.5	0.7	0.5116	0.0705	0.2962	0.7676	−0.0461	0.3325
	−0.5	0.5	0.5876	0.1301	0.3206	0.8090	−0.0346	0.3458
−0.75	0	1.0	0.7154	−0.0559	0.5855	0.9912	−0.2090	0.6384
	0	0.7	0.8123	−0.0517	0.6351	1.0467	−0.2169	0.6611
	0	0.5	0.8879	−0.0467	0.6715	1.0860	−0.2221	0.6769
	−0.25	1.0	0.5823	−0.1408	0.4568	0.8605	−0.3009	0.5137
	−0.25	0.7	0.6857	−0.1502	0.5128	0.9183	−0.3144	0.5385
	−0.25	0.5	0.7661	−0.1549	0.5539	0.9591	−0.3235	0.5556
	−0.5	1.0	0.4634	−0.1824	0.3417	0.7424	−0.3532	0.4029
	−0.5	0.7	0.5708	−0.2044	0.4009	0.8015	−0.3721	0.4287
	−0.5	0.5	0.6540	−0.2171	0.4438	0.8433	−0.3850	0.4465

borhood of a three-dimensional forward stagnation point under similarity assumptions can be expressed as[1,3]

$$f''' + (\omega - 1)g' f''/g + [(f + CF)f'' + g - f'^2]g^{1-\omega} = 0 \quad (1)$$

$$F''' + (\omega - 1)g' F''/g + [(f + CF)F'' + C(g - F'^2)]g^{1-\omega} = 0 \quad (2)$$

$$g'' + (\omega - 1)g'^2/g + Pr(f + CF)g' \, g^{1-\omega} = 0 \quad (3)$$

The appropriate boundary conditions are

$$f(0) = -f_w \qquad f'(0) = F(0) = F'(0) = 0$$

$$g(0) = g_w \qquad f'(\infty) = F'(\infty) = g(\infty) = 1 \quad (4)$$

where f and F are the dimensionless stream functions, g is the dimensionless enthalpy, g_w and $-f_w = (\rho w)_w/(\rho_e \mu_e a)^{1/2}$ are the dimensionless enthalpy and injection parameters at the wall, respectively, primes denote differentiation with respect to the independent similarity variable η, and subscripts w and e denote conditions at the wall and at the edge of the boundary layer, respectively (other symbols are given in Ref. 1). It may be noted that $\omega = 0.5$ corresponds to the conditions encountered in hypersonic flight, $\omega = 0.7$ corresponds to low-temperature flows, and $\omega = 1$ represents the constant density-viscosity product simplification.[2]

The skin-friction coefficients C_{f_x} and C_{f_y} along x and y directions and the heat-transfer coefficient in terms of the Stanton number St can be expressed as[1]

$$C_{f_x} = 2(Re_x)^{-1/2} f_1''(0)$$

$$C_{f_y} = 2(Re_x)^{-1/2} (v_e/u_e) F_1''(0) \quad (5)$$

$$St = (Re_x)^{-1/2} G'(0) \qquad f_1''(0) = g_w^{\omega - 1} f''(0)$$

$$F_1''(0) = g_w^{\omega - 1} F''(0) \quad (6)$$

$$G'(0) = Pr^{-1} g_w^{\omega - 1} g'(0)/(1 - g_w) \qquad Re_x = u_e x/\nu_e \quad (7)$$

Here $f_1''(0)$ and $F_1''(0)$ are the skin-friction parameters along x and y directions, respectively; $G'(0)$ is the heat transfer parameter and Re_x is the local Reynolds number.

Results and Discussion

Equations (1)-(3) under conditions (4) for both branches have been solved numerically using the method of parametric differentiation for various values C, ω, f_w, and g_w with $Pr = 0.7$. The detailed description of the method of parametric differentiation along with its application to various problems is given in Refs. 4-6. It has been observed from the results that the velocity profiles in the principal direction $f'(\eta)$ and the enthalpy profiles $g(\eta)$ for both branches for the saddle points of attachment ($C < 0$) are qualitatively the same for all values of ω, g_w, and f_w and are, therefore, not presented here. Some representative velocity profiles in the transverse direction $F'(\eta)$ for both discontinuous and continuous branches for $g_w = 0.2$ are shown in Fig. 1 (the velocity profiles for $g_w = 0.6$

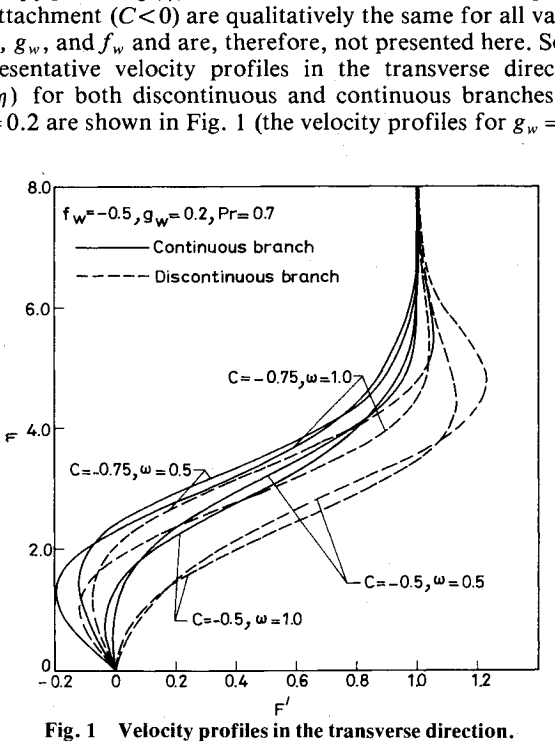

Fig. 1 Velocity profiles in the transverse direction.

are not shown here for lack of space‡). For the discontinuous branch, $F'(\eta)$ exhibits both reverse flow and velocity overshoot when $C=-0.75$ and $f_w=-0.5$ for all values of ω and g_w; there is no reverse flow when $C=-0.5$. Similar behavior has been observed by Libby[1] for $\omega=1$. For the continuous branch, the reverse flow occurs for both $C=-0.75$ and -0.5, but there is no velocity overshoot, for any value of C, ω, f_w, and g_w. The effect of decreasing ω from 1 to 0.5 is to decrease the reverse flow for both branches and to increase the velocity overshoot in the discontinuous branch (there is no velocity overshoot in the continuous branch). The effect is more pronounced for $g_w=0.2$ than for $g_w=0.6$. The occurrence of reverse flow and velocity overshoot is due to the combined effects of inertia, pressure, and shear in the boundary layer.[1] For both branches of solutions, the effect of increasing g_w is to increase the magnitude of reverse flow, whereas the effect of increasing f_w ($f_w<0$) or C ($C<0$) is to decrease it.

The skin-friction and heat-transfer parameters $f_l''(0)$, $F_l''(0)$, and $G'(0)$ for discontinuous branch for various values of the parameters are given in Table 1. The corresponding results for the continuous branch have also been obtained, but they are not given here for lack of space.‡ It is observed that $f_l''(0)$, $F_l''(0)$, and $G'(0)$ increase as ω decreases whatever may be the values of C, f_w, and g_w, but the effect of ω on them is more pronounced for lower values of g_w. For a given C, $f_l''(0)$, $F_l''(0)$, and $G'(0)$ decrease as f_w ($f_w<0$) decreases. It is also seen that $f_l''(0)$ and $G'(0)$ increases but $F_l''(0)$ decreases as C decreases and $F_l''(0)<0$ for some critical value of C depending on the magnitude of ω, f_w, and g_w. It may be noted that in the continuous branch the behavior of $f_l''(0)$ and $G'(0)$ for some values of f_w and g_w is opposite to that of the discontinuous branch until a critical value of C is reached for which $F_l''(0)=0$. Beyond this critical value of C, similar to the discontinuous case, $F_l''(0)$ and $G'(0)$ increase as C decreases. It is further observed that $f_l''(0)$ increases while $F_l''(0)$ decreases as g_w increases for all values of $\omega, C(C\leq -0.5)$, f_w ($f_w<0$), but $G'(0)$ increases or decreases as g_w increases depending on the values of C and f_w. We have compared our results for the continuous branch with those tabulated by Wortman et al.[2] and Vimala and Nath[3] and for the discontinuous branch (for $\omega=1$ and $g_w=0$§) with those tabulated by Libby[1] and found them to be in good agreement.

Conclusions

The skin friction both in the principal and transverse directions and heat transfer are significantly affected by the variation of the density-viscosity product ($\omega\neq 1$) across the boundary layer at low-wall temperatures. Furthermore, the skin friction in the transverse direction is strongly dependent on the nature of the stagnation point. The velocity profiles in the transverse direction exhibit both reverse flow and velocity overshoot, and the effect of the variation of the density-viscosity product is to decrease the reverse flow and to increase the velocity overshoot.

References

[1] Libby, P. A., "Heat and Mass Transfer at a General Three-Dimensional Stagnation Point," *AIAA Journal*, Vol. 5, March 1967, pp. 507-517.

[2] Wortman, A., Ziegler, H., and Soo-Hoo, G., "Convective Heat Transfer at General Three-Dimensional Stagnation Point," *International Journal of Heat and Mass Transfer*, Vol. 14, Jan. 1971, pp. 149-152.

[3] Vimala, C. S. and Nath, G., "Heat and Mass Transfer at a General Three-Dimensional Stagnation Point," *AIAA Journal*, Vol. 13, June 1975, pp. 711-712.

[4] Rubbert, P. E. and Landahl, M. T., "Solution of Nonlinear Problems through Parametric Differentiation," *Physics of Fluids*, Vol. 10, April 1967, pp. 831-835.

[5] Tan, C. W. and DiBiano, R., "A Parametric Study of Falkner-Skan Problem with Mass Transfer," *AIAA Journal*, Vol. 10, July 1972, pp. 923-925.

[6] Na, T. Y. and Turski, C. E., "Solution of Nonlinear Differential Equations for Finite Bending of a Thin-Walled Tube by Parametric Differentiation," *Aeronautical Quarterly*, Vol. 25, Feb. 1974, pp. 14-18.

‡The figure (results) can be obtained from the authors.

§The results are not tabulated here for the sake of brevity.

Improved Algebraic Relation for the Calculation of Reynolds Stresses

Z.U.A. Warsi* and B. B. Amlicke†
Mississippi State University, Mississippi State, Miss.

I. Introduction

THE prediction capability of a turbulence model depends on how effectively one can prescribe the Reynolds stress distribution in closing the system of equations. The simplest and most widely used has been the Boussinesq treatment of the Reynolds stresses. As is now well-known, the Boussinesq hypothesis holds only when the strain rates are fairly small. The main reason is that by construction the Boussinesq formula implies that the principal axes of the Reynolds stress tensor are parallel to the principal axes of the strain rate tensor, so that any change in the strain rate is directly felt in the stresses. This instantaneous change of the Reynolds stresses with the strain rates is not supported by the experimental observations, because the Reynolds stresses, being due to the vorticity fluctuations, require some time to adjust to the new strain rates. In order to overcome these shortcomings, one must either abondon the Boussinesq hypothesis altogether and solve the six Reynolds transport equations, which is costly in terms of computer time, or improve upon the hypothesis itself.

In this paper, we follow a recent analysis of Rodi[1] to construct an improved second-order version of the Boussinesq hypothesis. An algebraic relation for the turbulent stresses has been obtained through a consideration of the transport equations of the Reynolds stresses. Consequently, the resulting relation has the necessary influence of the convective and diffusive transport effects of a turbulence stress field.

II. Analysis

The transport equations of the Reynolds stresses ($-\overline{u_i u_j}$) and the equation of turbulence energy ($\bar{e}=\frac{1}{2}\overline{u_i u_i}$) for an incompressible flow, respectively, are

$$d\tau_{ij}/dt = P_{ij} + Q_{ij} + D_{ij} - \epsilon_{ij}, \quad \tau_{ij} = \overline{u_i u_j} \tag{1}$$

$$d\bar{e}/dt = P + D - \epsilon \tag{2}$$

where d/dt is the substantive derivative based on the mean velocity components U_i; P_{ij}, D_{ij}, ϵ_{ij}, respectively, are the production, diffusion, and dissipation of the Reynolds stresses, Q_{ij} is the pressure-strain correlation, and P, D, and ϵ, respectively, are the production, diffusion, and dissipation of the turbulence energy. In this paper, we have used the modeling of the terms Q_{ij}, D_{ij}, ϵ_{ij}, and D as reported in Refs. 1 and 2, which, when using the summation convention on

Received July 6; revision received Sept. 7, 1976. This paper is an outgrowth of current research supported by the U.S. Air Force Office of Scientific Research, Grant No. AFOSR-76-2922.

Index category: Boundary Layers and Convective Heat Transfer – Turbulent.

*Associate Professor, Aerophysics and Aerospace Engineering.

†Graduate Research Assistant.